Materials Today Sustainability 21 (2023) 100302

Contents lists available at ScienceDirect

Materials Today Sustainability

journal homepage: https://www.journals.elsevier.com/materials-today-sustainability

Synthesis of SAPO-34 by utilizing spent industrial MTO catalyst and their catalytic applications

Z. Liu [a, b], Q. Wang [b], S. Liu [b], M. Yang [b], D. Fan [b], D. Zhu [b, c], P. Tian [b, *], Z. Liu [b, **]

[a] Green Catalysis Center, College of Chemistry, Zhengzhou University, Zhengzhou, 450001, China
[b] National Engineering Research Center of Lower-Carbon Catalysis Technology, Dalian National Laboratory for Clean Energy, Dalian Institute of Chemical Physics, Chinese Academy of Sciences, Dalian, 116023, China
[c] University of Chinese Academy of Sciences, Beijing, 100049, China

ARTICLE INFO

Article history:
Received 12 August 2022
Received in revised form
22 December 2022
Accepted 25 December 2022
Available online 30 December 2022

Keywords:
SAPO-34
Molecular sieve synthesis
Spent MTO catalyst
Methanol to olefins
Methanol ammoniation

ABSTRACT

The methanol-to-olefins (MTO) process has realized its large-scale industrialization over the past decade. The corresponding consumption of MTO catalyst is currently more than 10,000 tons per year. To convert the spent industrial MTO catalyst into valuable materials would be significant for environment protection and for the development of MTO industry. Here, the spent industrial MTO catalyst was utilized as raw material to explore the synthesis of SAPO-34 and their catalytic applications. Two amines with different sizes including diethylamine (DEA) and tetraethylammonium hydroxide (TEAOH) were employed as the synthesis templates. It was found that the Si/Al/P sources in spent MTO catalyst have high reactivity and SAPO-34 with varied Si contents can be synthesized in high crystallinity. Low-silica SAPO-34 exhibits good catalytic performance in the MTO reaction. More importantly, compared with SAPO-34-TEAOH, SAPO-34-DEA shows excellent catalytic performance in the methanol ammoniation reaction with high selectivity to methylamine (MMA) and dimethylamine (DMA) due to its higher acid concentration and larger crystal size. After hydrothermal treatment of SAPO-34-DEA at 800 °C, although the methanol conversion shows a decrease (~25% drop), the MMA plus DMA selectivity in three methylamines increases to as high as 94%.

1. Introduction

Last decade has witnessed the rapid development and industrialization of the methanol-to-olefins (MTO) process, which provides an efficient way to produce ethene and propene from non-oil resources such as coal and natural gas [1–5]. Hitherto, several MTO technologies with the use of fluidized bed reactor have been commercialized including DMTO technology of Dalian Institute of Chemical Physics (DICP), UOP/Hydro MTO process and SMTO technology of Shanghai Research Institute of Petrochemical Technology (SRIPT) [6]. The total olefins production capacity of the MTO commercial units currently achieves more than 16 Mt/a in China, and about half of them are produced from DMTO process. The corresponding consumption of MTO catalyst is more than 10,000 tons per year. However, the spent industrial MTO catalysts are classified as hazardous waste, which requires special disposal to avoid its potential threats to the environment. It is thus of great significance to carry out the research on the utilization of spent MTO catalysts, refreshing or converting them to high-value materials.

SAPO-34 molecular sieve with 8-membered ring channels and CHA nanocages is the active component of industrial MTO catalyst, owing to its superior light olefins selectivity and high-temperature hydrothermal stability [6–10]. Besides as MTO catalyst, SAPO-34 exhibits good catalytic performance in the methanol ammonination reaction [11–13]. Moreover, Cu/SAPO-34 has also been recognized as promising catalyst for the NH_3-SCR reaction [14–17]. It has been demonstrated that the catalytic performance of SAPO-34 is closely related with its acidity, which is indeed determined by Si content and Si coordination environment in the framework. To achieve satisfied acidity, besides controlling the Si content in the initial gel, the template used for the synthesis of SAPO-34 is also crucial [18–21]. With the use of organic amines with smaller size (DEA, morpholine, etc.), more than one template molecule are generally accommodated in one CHA cage, which can balance more

* Corresponding author.
** Corresponding author.
E-mail addresses: tianpeng@dicp.ac.cn (P. Tian), zml@dicp.ac.cn (Z. Liu).

https://doi.org/10.1016/j.mtsust.2022.100302
2589-2347/

negative framework charges and lead to a product with higher Si content and more Si(4Al) species [22,23]. When organic amines with larger volume, such as TEAOH and triethylamine, are used as template, one CHA cage can only contain one template molecule, which facilitates the synthesis of low-silica SAPO-34 or SAPO-34 with diverse Si coordination environments (corresponding to the formation of Si islands) [14,20].

The industrial MTO catalyst for fluidized bed reactor has spherical morphology with mediate diameter of 80–90 μm [2,24,25]. It is mainly composed of silica, alumina and phosphorus oxide, which can provide all three inorganic sources required for the synthesis of SAPO molecular sieves. In addition, the structure of SAPO-34 may be partially maintained in the spent catalyst, which can play as seeds and would be beneficial for the crystallization of SAPO-34. In this work, we explore the synthesis of SAPO-34 molecular sieves by utilizing spent industrial MTO catalyst as raw material. Two organic amines (TEAOH and DEA) with different sizes were employed as the template. The resultant products were characterized in detail. In addition, the catalytic performances of the samples for the MTO reaction and methanol ammoniation reaction were studied and discussed.

2. Experimental section

2.1. Materials

The spent industrial MTO catalyst was from the commercial DMTO units. It was calcined at 650 °C to remove the residual carbon before use. The elemental composition of the spent MTO catalyst is listed in Table 1. The chemical reagents used for the syntheses include: silica sol (27.5 wt%), phosphoric acid (H_3PO_4, 80 wt%), pseudo-boehmite (Al_2O_3, 67.5 wt%), diethylamine (DEA, 99.5 wt%) and tetraethylammonium hydroxide (TEAOH, 35 wt%). They are all commercial reagents and used without purification.

2.2. Hydrothermal synthesis

The syntheses of SAPO-34 using spent MTO catalyst were carried out using DEA or TEAOH as the template. Scheme 1 illustrates the synthesis process of SAPO-34. The detailed amounts of sources for the syntheses are shown in Table 2. A typical synthesis procedure can be described as follows: the spent MTO catalyst was first calcined to remove the carbon deposition and was added into the beaker followed with the addition of deionized water, pseudo-boehmite (if needed), phosphoric acid and silica sol (if needed) under stirring. After 20 min of stirring, organic template was added into the mixture and stirred for 20 min. The final mixture was loaded into 100 mL stainless steel reactor and crystallized at certain temperature for 24 h under rotation (40 rpm). After the crystallization was completed, solid product was separated by centrifugation, washing and drying. The as-synthesized solid was calcined at 650 °C for 3 h to remove the organics and obtain H-form sample.

2.3. Characterization

PANalytical X'Pert PRO X-ray diffractometer was used to measure X-ray diffraction (XRD) patterns of the samples, which uses Cu Kα radiation (λ = 1.5418 Å) at 40 mA and 40 kV. Elemental composition was measured using a PANalytical AXios X-ray fluorescence (XRF) spectrometer. Scanning electron microscopy (SEM) images of the samples were acquired with the Hitachi TM 3000 benchtop scanning electron microscope and the Hitachi SU8020 scanning electron microscope. ASAP 2020 gas adsorption analyzer was used for N_2 physisorption test at −196 °C (samples were pretreated in vacuum at 350 °C for 6 h). The surface elemental compositions of the samples were measured using Thermo fisher Escalab 250 Xi + X-ray photoelectron spectroscopy (XPS). Thermogravimetry analysis (TGA) was conducted by a TA SDT Q-600 analyzer under 100 mL/min of air flow with a heating rate of 20 °C/min. NH_3-TPD were determined by Micromertics Autochem Model 2920 Chemisorber. Prior to the measurements, 0.1 g of calcined sample was pretreated under He at 650 °C for 1 h. Then, the sample was cooled down to 100 °C, exposed in NH_3 (2% NH_3 in He) for 0.5 h and purged by He for 1 h to remove physically adsorbed NH_3. The measurement was conducted from 100 to 600 °C with a heating rate of 10 °C/min under He flow (30 mL/min). FT-IR spectrum of calcined sample was recorded using a Fourier transform infrared spectrometer (Brukers XF808-04). Before the measurement, the sample was in situ pretreated in vacuum at 350 °C for 2 h.

Table 1
Elemental composition of the spent MTO catalyst.

Composition	SiO_2	Al_2O_3	P_2O_5	Others
wt%	26.4	50.8	21.2	1.6

All solid-state NMR experiments were conducted using a 4 mm MAS probe over Bruker Avance III 600 spectroscopic instrument equipped with a 14.1 T wide-aperture magnet. The ^{27}Al MAS NMR spectra were recorded with a pulse sequence. The π/8 pulse width was 0.75 μs, the cycle delay was 2 s, and the chemical shift was referenced to 0.4 ppm $(NH_4)Al(SO_4)_2{\cdot}12H_2O$. The ^{31}P MAS NMR spectra were recorded by high-energy proton decoupling technique, with a π/4 pulse width of 2.25 μs, a cycle delay of 10 s. The chemical shift of ^{31}P was referenced to 85% H_3PO_4 at 0 ppm. The ^{29}Si MAS NMR spectra were recorded with a contact time of 3 ms, a cycling delay of 2 s, and a rotation rate of 8 kHz. The chemical shift of ^{29}Si was referenced to −91.5 ppm kaolinite.

2.4. MTO reaction

The MTO reactions were conducted in a quartz fixed-bed reactor. 0.3 g of calcined catalyst (40–60 mesh) was loaded into the reactor, activated at 500 °C for 2 h with N_2 (42 mL/min), and then reduced to the reaction temperature (450 °C). Methanol vapor was fed into the reactor using N_2 gas (42 mL/min) as carrier. The weight hourly space velocity (WHSV) of methanol was 3.65 h^{-1}. The reaction products were analyzed by using online gas chromatograph (Agilent 7890, Pora PLOT Q-HT column, FID detector). The products selectivity was determined by mass percent and dimethyl ether was calculated as reactant. Reaction lifetime was defined as the duration of methanol conversion over 99%.

2.5. Methanol ammoniation reaction

0.3 g of calcined catalyst (40–60 mesh) was loaded in a stainless steel fixed-bed reactor, activated at 370 °C for 1 h in N_2, and then reduced to the reaction temperature of 320 °C. NH_3 was first introduced in the reactor. After 5 min, methanol vapor was fed in the reactor using N_2 gas (25.3 mL/min) as carrier. The WHSV of methanol was 0.813 h^{-1}. The NH_3/methanol molar ratio in the feed was 2:1. The products were analyzed by using online gas chromatograph (Agilent 7890, CPVolamine column, FID detector).

3. Results and discussion

3.1. Characterization of the spent industrial MTO catalyst

The elemental composition of the spent MTO catalyst is displayed in Table 1, which contains SiO_2, P_2O_5 and Al_2O_3 as the major

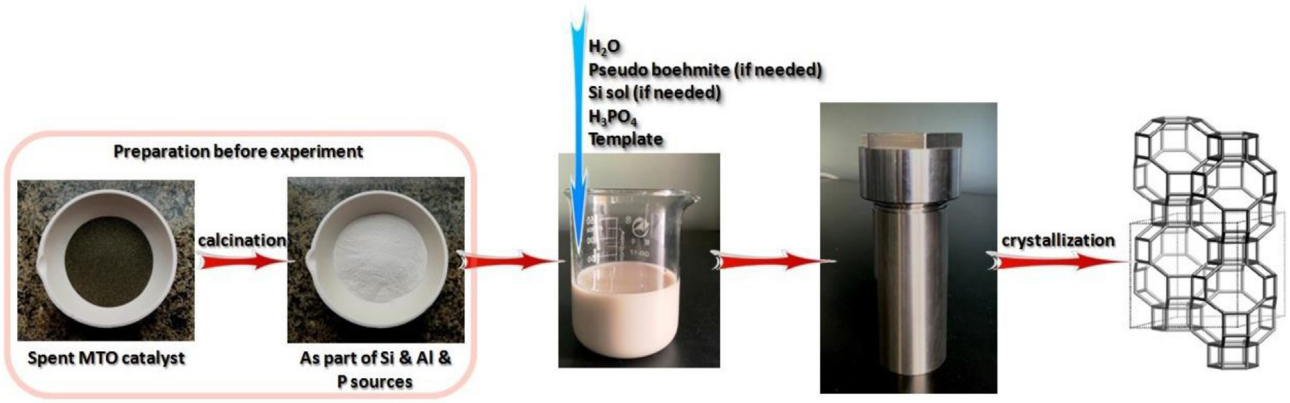

Scheme 1. Schematic procedure for SAPO-34 synthesis using spent industrial MTO catalyst as raw sources.

components (about 98.4%). Fig. 1 displays the XRD pattern and SEM images of the calcined spent catalyst. Weak XRD peaks ascribed to the CHA structure can be observed, implying the partial maintaining of SAPO-34 framework in the spent catalyst. Moreover, the SEM images show that the spent catalyst consists of broken spherical particles in sizes of 2−30 μm. Further magnification reveals the existence of cubic crystals (about 3 μm) in the particles, which is the typical morphology of SAPO-34. The MTO catalytic performance of the calcined spent catalyst was also evaluated and indicated in Fig. S1. The observed short catalytic lifetime together with low ethene plus propene selectivity suggests the destroyed crystal structure of SAPO-34, consistent with the XRD results.

3.2. Synthesis and characterization of SAPO-34 by using the spent MTO catalyst and DEA template

The synthesis of SAPO-34 with the use of spent MTO catalyst is first explored by using DEA as a template. The detailed synthesis conditions, product compositions and solid yields are shown in Table 2. The XRD patterns of the as-synthesized products are given in Fig. 2. When the x(SiO_2) amount in the initial gel is at 0.38 or lower, SAPO-34 product with small amount of impurity (AWO framework) would be obtained, as indicated by the weak peak at 10.1° in the XRD pattern [26]. Further increasing the initial x(SiO_2) to 0.55 and 0.90, SAPO-34 in high purity and increased yield can be readily synthesized. The Si incorporation level of the syntheses is also listed in Table 2, showing a gradual decrease with the increase of initial Si content. Compared with our previous work [23] about the synthesis of SAPO-34 using DEA template and conventional Si/Al/P sources at 200 °C, samples D-10 and D-15 show comparable Si incorporation levels, while for sample D-20, its Si incorporation is obviously higher than that of the conventional synthesis with similar initial gel composition. These results imply that the present synthesis route with DEA template facilitates the achievement of high-silica SAPO-34, which is likely due to the high-silica character of the spent MTO catalyst.

The SEM images (Fig. 2) show that all the samples have typical rhombohedral morphology, and no amorphous materials can be observed. The average grain size of the samples presents a decreasing trend following the increase of product Si content. This phenomenon may be owing to the change of Si environments (Fig. 3), as the formation of Si islands affects the T-O-T bond angle/length in the SAPO framework and thus the growth of crystals [14,27]. The textural properties determined by N_2 sorption measurements are listed in Table 3. The micropore surface area and micropore volume of sample D-10 are slightly lower than those of D-15 and D-20, likely due to the existence of impurity. The values of D-15 and D-20 are close to those previously reported, implying the good quality of the synthesized SAPO-34.

XPS analysis was performed to measure the surface composition of the samples. As shown in Table 2, the surface Si contents are higher than those of the bulk, indicating an increased Si content from the core to the shell. Such Si enrichment phenomenon aggravates from D-10 to D-20. These findings are consistent with previous reports on SAPO-34 and many SAPO molecular sieves, implying inhomogeneous spatial distribution of Si atoms (acid sites) in the crystals [28]. The thermal analysis curves of the samples are presented in Fig. S2, showing a weight loss of 12.7−13.3% in the temperature range of 200−750 °C due to the removal of organics. The average number of template per CHA cage is calculated to be about 1.6 DEA for the samples.

Table 2
Synthesis conditions, product compositions and yields of the samples synthesized using spent MTO catalyst.

Sample[a]	Gel					Product		Si incorporation[b]	$Si_{surface}/Si_{bulk}$[c]
	x SiO_2 (mol)	Spent catalyst addition	Added Si/Al/P sources			Composition (in mole)	Yield (%)		
			H_3PO_4	Al_2O_3	Si sol				
D-10	0.38	4.32 g	8.23 g	4.28 g	0	$Si_{0.115}Al_{0.503}P_{0.382}$	81.6	1.32	1.20
D-15	0.55	6.25 g	9.97 g	2.81 g	0	$Si_{0.147}Al_{0.489}P_{0.365}$	83.0	1.21	1.29
D-20	0.90	9.96 g	8.62 g	0	0.26 g	$Si_{0.216}Al_{0.461}P_{0.323}$	94.4	1.17	1.46
T-10	0.40	4.54 g	10.59 g	4.11 g	0	$Si_{0.102}Al_{0.498}P_{0.399}$	57.4	1.20	1.07
T-15	0.60	6.82 g	9.77 g	2.38 g	0	$Si_{0.153}Al_{0.475}P_{0.372}$	83.0	1.17	1.54
T-20	0.86	9.77 g	8.69 g	0.14 g	0	$Si_{0.199}Al_{0.458}P_{0.344}$	–	1.12	–

[a] Final gel molar composition for D-10, D-15 and D-20: xSiO_2: 0.8P_2O_5: 1Al_2O_3: 50H_2O: 2DEA (200 °C, 24 h), for T-10, T-15 and T-20: xSiO_2: 1P_2O_5: 1Al_2O_3: 50H_2O: 2TEAOH (210 °C, 24 h).
[b] Si incorporation = [Si/(Si + Al + P)]product/[Si/(Si + Al + P)]gel.
[c] [Si/(Si + Al + P)]surface/[Si/(Si + Al + P)]bulk, the surface and bulk compositions were determined by XPS and XRF, respectively.

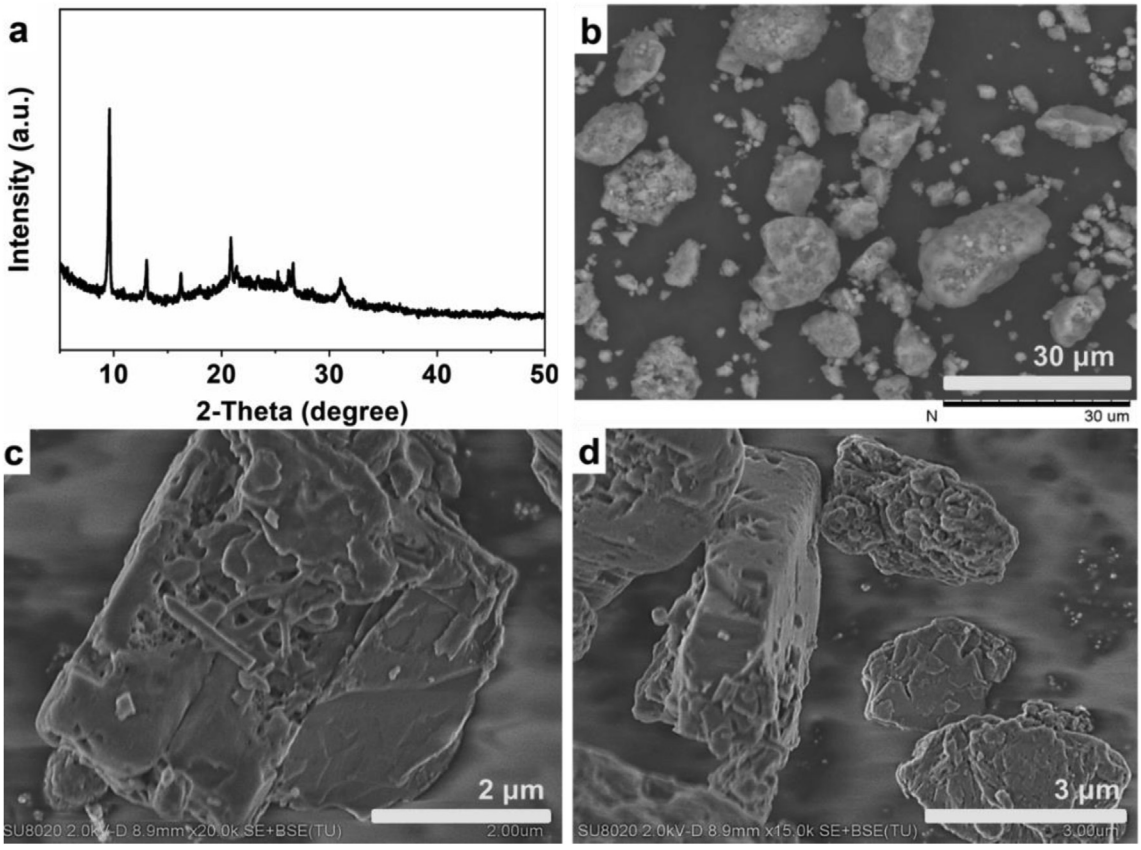

Fig. 1. XRD pattern (a) and SEM images (b–d) of the spent MTO catalyst.

The local atomic environments in the SAPO-34 samples were investigated by ^{29}Si, ^{31}P and ^{27}Al MAS NMR spectra. Fig. 3 displays the ^{29}Si spectra of the samples. The resonance signals at −91, −95, −101, −106, and −110 ppm can be ascribed to Si(4Al), Si(3Al), Si(2Al), Si(1Al) and Si(0Al) species, respectively. For sample D-10, one strong resonance at −91 ppm can be observed in the spectrum, showing the dominant existence of Si(4Al) species in the SAPO framework. With the increase of product Si content, the ^{29}Si spectrum becomes complex and indicates the formation of Si islands. Especially for sample D-20, all five Si species could be clearly observed. This is reasonable as the maximum framework charges are determined by the incorporated template in the CHA cage. Based on the above finding of 1.6 DEA per CHA cage, the maximum threshold of Si content for the formation of Si islands is calculated to be about 13.3%. At higher Si amount, the formation of Si islands would be necessary in order to reach the charge balance. Moreover, samples D-10 and D-15 have comparable Si environments to the SAPO-34 synthesized from conventional sources and with approximate Si contents [23,29], which suggests that the use of spent catalyst as raw material has less impact on the product Si environments.

The ^{27}Al MAS NMR spectra are illustrated in Fig. S3, in which three signals can be observed for all three samples. The strong resonance around 38 ppm can be attributed to tetrahedral framework Al species, while the signals at 12 ppm and −8 ppm correspond to penta- and hexa-coordinated Al species, respectively. The ^{31}P spectra of the samples are shown in Fig. S4. Only one strong resonance at −29 ppm appears in the three spectra, evidencing the dominant existence of P(4Al) species in the framework.

3.3. Synthesis and characterization of SAPO-34 by using the spent MTO catalyst and TEAOH template

The syntheses of SAPO-34 with the use of spent MTO catalyst and TEAOH template were carried out at 210 °C for 24 h. The detailed synthesis information is given in Table 2. The XRD patterns of the as-synthesized products are shown in Fig. 4. Sample T-10 possesses pure CHA structure, but with lower solid yield. For samples T-15 and T-20 with higher Si contents, the decreased relative peak intensity at 20.6°, the broadened peak at 25.° and the appearance of new weak sharp peak at 26.7° in the XRD patterns suggest that their structures may contain small amount of AEI intergrowth [30].

The SEM images (Fig. 4) reveal that all the samples consist of crystallites in sizes of 100–300 nm, obviously smaller than those of the SAPO-34 templated by DEA [31,32]. This should be owing to the higher nucleation ability of TEAOH. Note that the crystal sizes herein are close to those of SAPO-34 synthesized from TEAOH template and conventional inorganic sources. In addition, as presented in Table 3, the three samples possess comparable and large micropore surface areas and micropore volumes, confirming their good crystallinity. They have larger external surface areas and mesopore volumes than SAPO-34 templated by DEA, which are consistent with their smaller crystal sizes.

The XPS results listed in Table 2 reveal that sample T-10 has comparable surface Si content to that of the bulk. However, the surface Si enrichment becomes evident following the increase of product Si content. The thermal analysis results are given in Fig. S2, from which the average number of TEA^+ per CHA cage is calculated to be one for the samples.

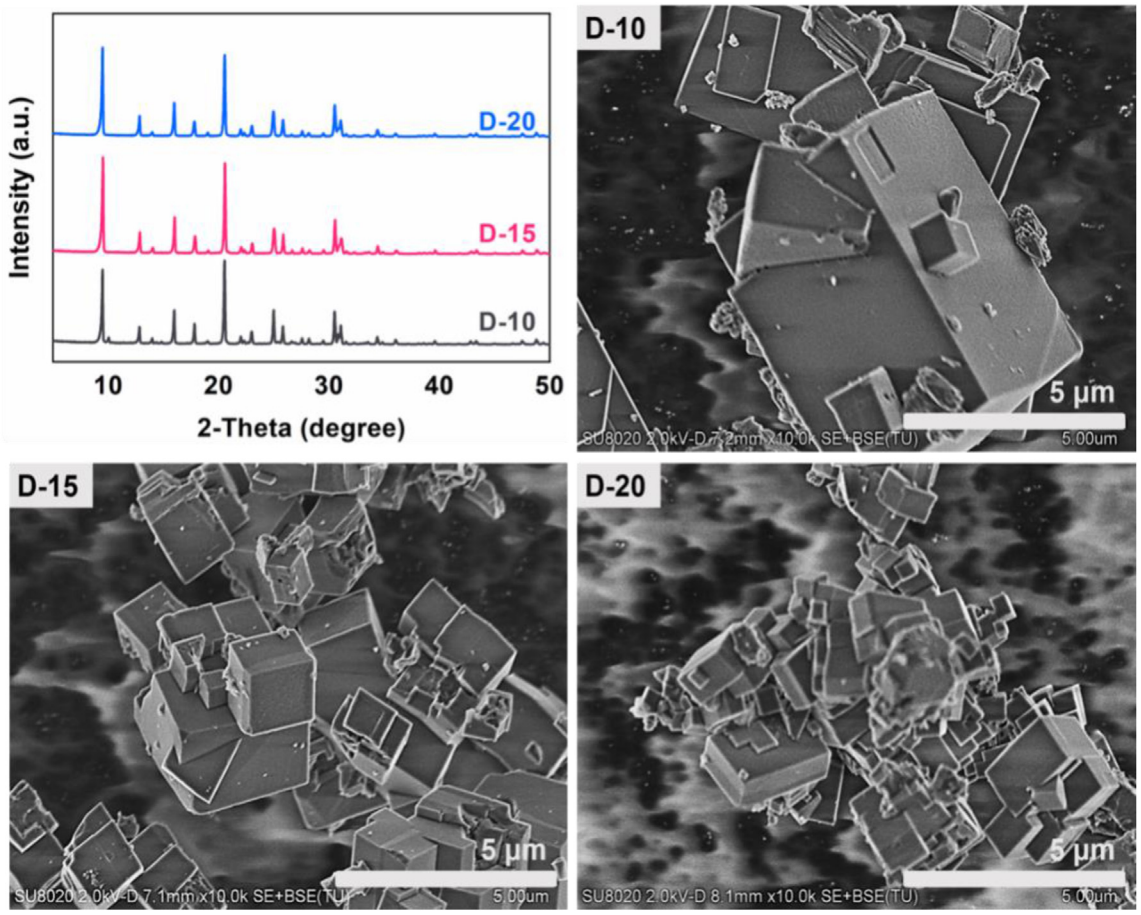

Fig. 2. XRD patterns and SEM images of the SAPO-34 synthesized using DEA template.

The ^{29}Si MAS NMR spectra of the samples are shown in Fig. 3. For sample T-10, besides the strong resonance at −92 ppm, there are obvious signal around −96 ppm and weak signal at −110 ppm, suggesting the appearance of Si islands in the framework. This agrees with the above finding about one TEA^+ cation per CHA cage, corresponding to a threshold of Si content of about 8.3% for the formation of Si islands. The deconvoluted results of the samples are displayed in Table S1. Following the increase of product Si content, the Si coordination environments become complex, and the proportion of Si islands rises at the expense of Si(4Al) species. The Si environments of the samples are basically similar to those of conventional SAPO-34 templated by TEAOH with approximate Si content [14]. Fig. S3 presents the ^{27}Al MAS NMR spectra of the samples, which have strong resonance at 38 ppm and weak signals at 11 ppm, corresponding to tetrahedral and pentahedral Al species, respectively. The content of pentahedral Al species show a decreasing trend following the incremental Si content. The ^{31}P spectra are given in Fig. S4, indicating the sole existence of P(4Al) species in the framework of the three samples.

3.4. Acidity of the SAPO-34 samples

The acidity of the SAPO-34 samples with different Si contents was investigated by NH_3-TPD. Figs. S5 and S6 illustrate the NH_3-TPD profiles and the deconvoluted curves, respectively. The detailed acid distributions are listed in Table 4. It is clear that the proportion of strong acid sites increases following the incremental Si content for both serial samples, which agree well with the increased proportion of Si island species (Fig. 3). The overall acid amounts of SAPO-34 templated by DEA are larger than those of SAPO-34 templated by TEAOH, which are reasonable as the former samples have higher template numbers per CHA cage and larger proportion of Si(4Al) species. For SAPO-34-DEA samples, D-15 and D-20 have comparable (M + S) acid amounts, which are larger than those of D-10. For SAPO-34-TEAOH samples, three of them possess approximate (M + S) acid amounts, lower than those of SAPO-34-DEA samples.

3.5. Catalytic performance in the MTO reaction

The MTO catalytic performance of SAPO-34 synthesized by using spent MTO catalyst as the main raw material was tested. As shown in Fig. S7, low-silica SAPO-34 catalysts, whatever the template employed, show better catalytic performance than high-silica ones, which are reasonable as previous works have demonstrated that SAPO-34 with lower Si content and Si(4Al) species (corresponding to lower acid concentration and acid strength) facilitates the MTO reaction [2]. Fig. 5 presents the catalytic results of low-silica samples D-10 and T-10. From Fig. 5a, sample T-10 has a long catalytic lifetime of 276 min (methanol conversion >99%) under the investigated conditions, which is about twice than that on sample D-10. The selectivity of ethene plus propene rises with time on stream and reaches the maximum value of 82.2% on T-10 and 86.2%

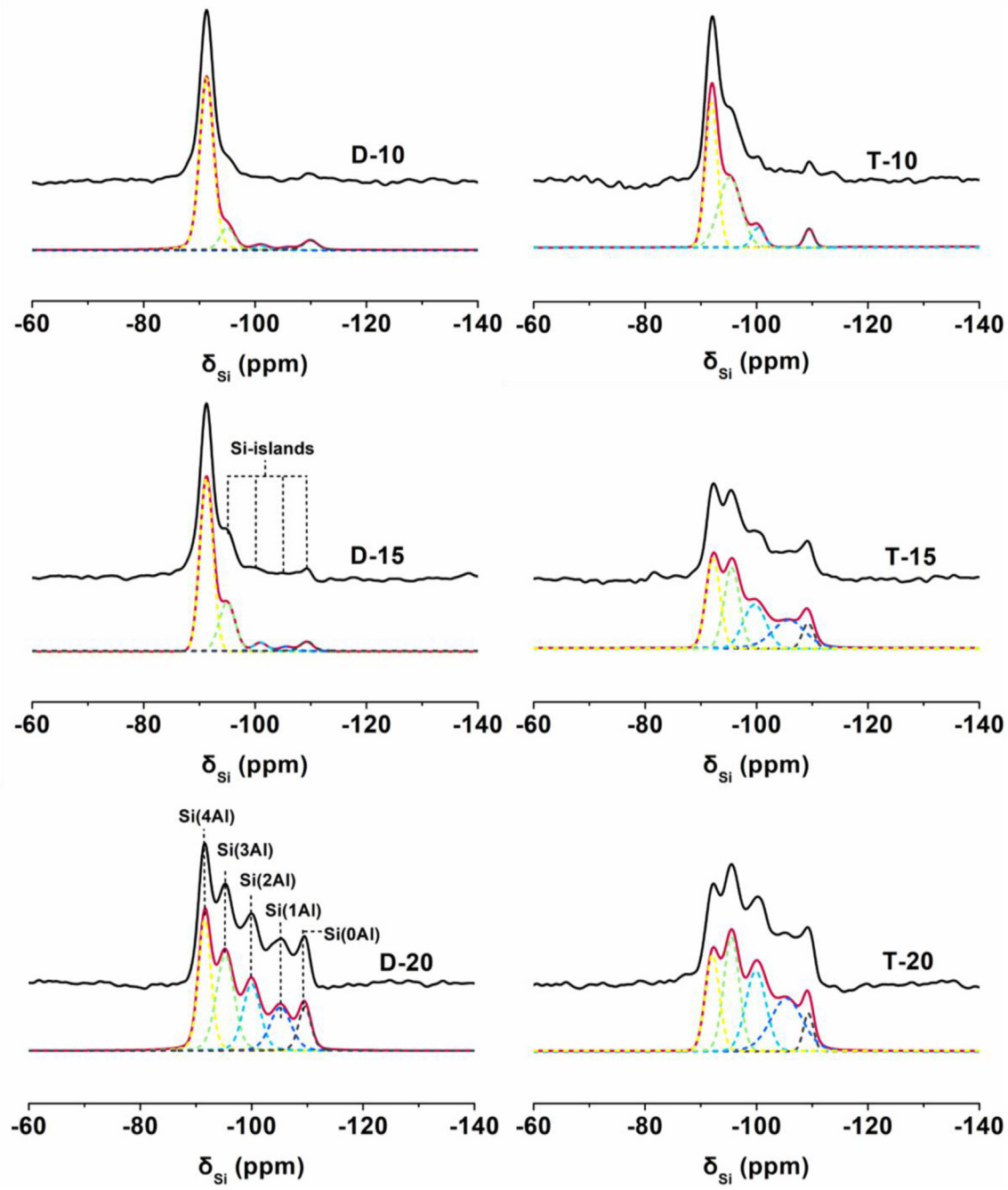

Fig. 3. ^{29}Si MAS NMR spectra of the as-synthesized SAPO-34 samples.

Table 3
Textural properties of the SAPO-34 samples.

Sample	Pore volume[a] (cm^3/g)			Surface area[b] (m^2/g)		
	V_{total}	V_{micro}	V_{meso}	S_{total}	S_{micro}	S_{ext}
D-10	0.23	0.22	0.01	454	449	5
D-15	0.26	0.25	0.01	515	512	4
D-20	0.25	0.24	0.01	494	481	13
T-10	0.31	0.25	0.06	532	501	31
T-15	0.33	0.24	0.09	546	493	53
T-20	0.32	0.24	0.08	531	485	46

[a] V_{total} is evaluated at $P/P_0 = 0.97$; V_{micro}: t-plot micropore volume; $V_{meso} = V_{total} - V_{micro}$.
[b] S_{total}: BET surface area; S_{micro}: t-plot micropore surface area; $S_{ext} = S_{total} - S_{micro}$.

on D-10 before the catalyst deactivation. It is speculated that the relatively low acid concentration and small crystal size of T-10 contributes to its longer lifetime, which are consistent with the obviously low hydrogen transfer index (HTI) on it. Moreover, the distinct selectivity of ethene plus propene on D-10 and T-10 should be owing to their difference in the micro-structures, as evidenced by the XRD patterns of the two samples. Indeed, our previous works have revealed that the unit cells of SAPO-34 vary slightly with the templates employed [33]. Furthermore, SAPO-34 containing small amount of SAPO-18 intergrowth would also cause lower selectivity of ethene plus propene, as the relatively larger AEI cage of SAPO-18 can allow the formation of larger active intermediates, leading to the variation of product selectivity [34].

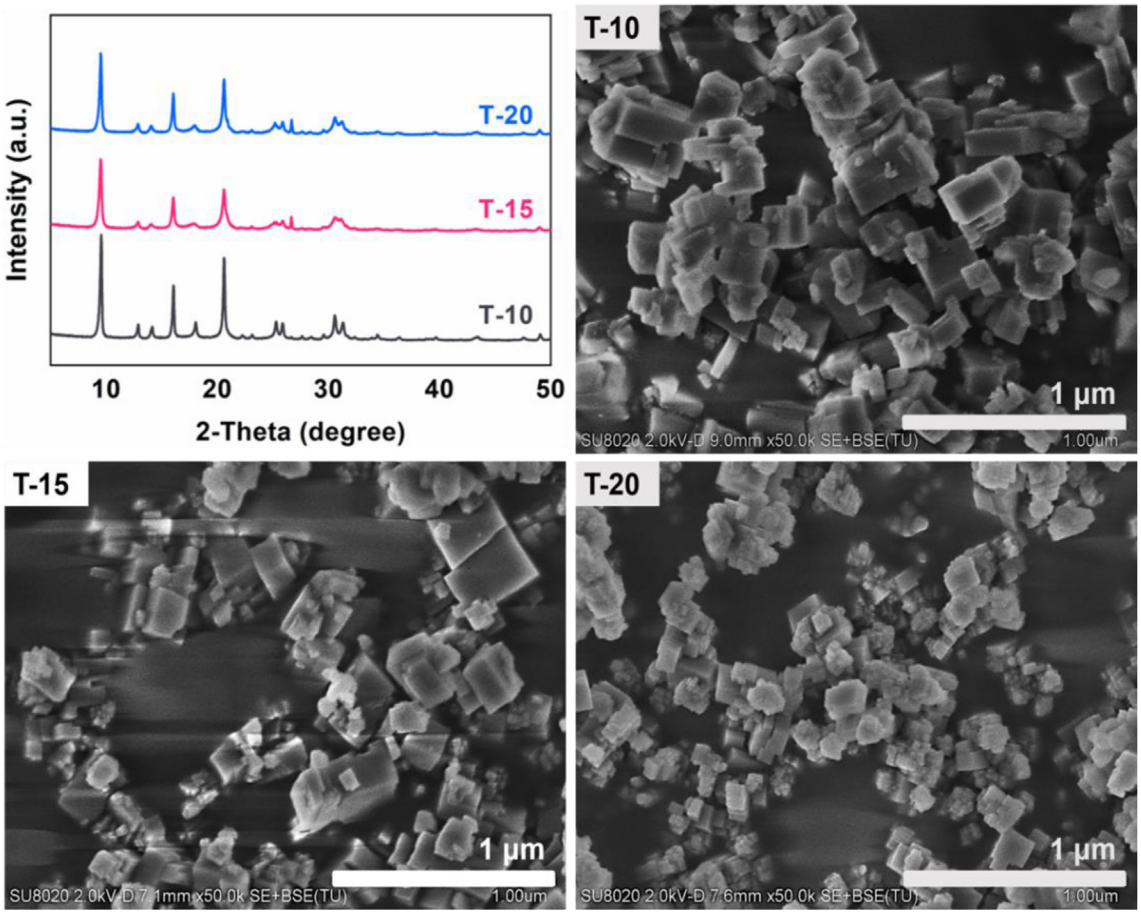

Fig. 4. XRD patterns and SEM images of the SAPO-34 synthesized using TEAOH template.

3.6. Catalytic performance in the methanol ammoniation reaction

Methylamine (MMA) and dimethylamine (DMA) are valuable chemical intermediates, which are primarily manufactured by the methanol amination reaction using amorphous SiO_2—Al_2O_3 as the catalyst. However, trimethylamine (TMA) is the dominant product during this process due to thermodynamic equilibrium. Small pore 8-MR molecular sieves have been demonstrated to be promising catalysts with improved selectivity for MMA and DMA [11,35]. Herein, the synthesized SAPO-34 samples were tested as the catalyst for the methanol amination reaction. Fig. 6 and S8 reaction results of the samples. SAPO-34-DEA samples show a gradual increase of methanol conversion from D-10 to D-20, implying that both large acid amounts and high acid strength facilitate the methanol conversion. The dominant products over the three catalysts are DMA, followed by MMA, TMA and dimethylether (DMM). Remarkably, sample D-20 possesses the highest DMA selectivity of about 60% and the lowest selectivity to TMA and DME. For SAPO-34-TEAOH samples, they show comparable methanol conversion to the corresponding SAPO-34-DEA samples. Nevertheless, they yield much more TMA (40–45% selectivity) than DMA and MMA, significantly different from SAPO-34-DEA and our previous reports [13]. This should result from the small crystal sizes and large external surface areas of SAPO-34-TEAOH, as the abundant acid sites on the external surface can further catalyze the methylation of DMA and MMA diffused from the 8-MR channels. Pyridine-adsorbed FTIR spectra were measured to learn the external acid properties of the samples (Fig. 7a), as the kinetic diameter of pyridine is too large to enter the 8-MR channels of SAPO-34. Clearly, SAPO-34-DEA samples possess very weak external surface acidity, while T-20 has relatively large amount of Brønsted and Lewis acid sites on the external surface.

Table 4
The relative acid amounts of the samples determined from NH_3-TPD.

Sample	Acid sites distribution[a] (%)			Total (%)	M + S[b] (%)
	Weak acid	Moderate acid	Strong acid		
D-10	35.8	29.5	18.2	83.5	47.6
D-15	43.7	33.9	22.4	100.0	56.3
D-20	42.6	26.5	29.3	98.3	55.8
T-10	30.0	24.6	15.6	70.2	40.2
T-15	28.8	22.4	17.5	68.7	39.9
T-20	28.8	21.5	18.1	68.3	39.6

[a] The peak temperatures in the NH_3-TPD profiles for the weak, moderate and strong acid sites are around 198 °C, 380 °C and 460 °C, respectively.
[b] The sum of moderate and strong acid sites.

In order to learn the long-term stability of the samples for methanol amination reaction, sample D-20 with the best catalytic conversion and DMM selectivity was selected for high-temperature hydrothermal treatment under 100% steam at 700 °C and 800 °C. The NH_3-TPD profiles of the samples are shown in the Fig. 7b. It can be found that hydrothermal treatment significantly reduces the acid amount and acid strength of the sample and the decreasing trend rises with the increase of treatment temperature. The amination reaction results of the samples after hydrothermal treatment are presented in Table 5. The conversion drops with the

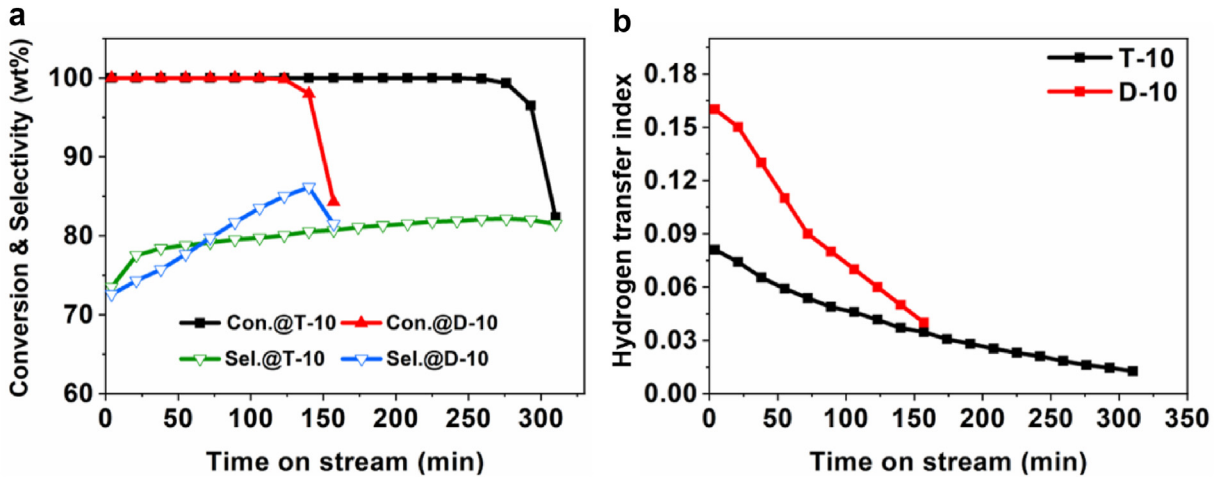

Fig. 5. (a) Methanol conversion, selectivity of ethene plus propene and (b) hydrogen transfer index (C_3H_8/C_3H_6) in the MTO reaction over sample D-10 and T-10. Reaction conditions: 450 °C, methanol WHSV = 3.65 h^{-1}.

incremental treatment temperature, consistent with the decreased acid amounts of the samples. About 65% of methanol conversion can still be maintained on D-20-800 °C sample. Moreover, although the DME selectivity rises following the incremental treatment temperature, the (MMA + DMA) selectivity in the three methylamine products presents an increased trend, which can reach as high as 94% on D-20-800 °C. These results demonstrated that SAPO-34 synthesized by using spent catalyst and DEA template has high activity, stability and selectivity to DMM and MMA for the methanol amination reaction.

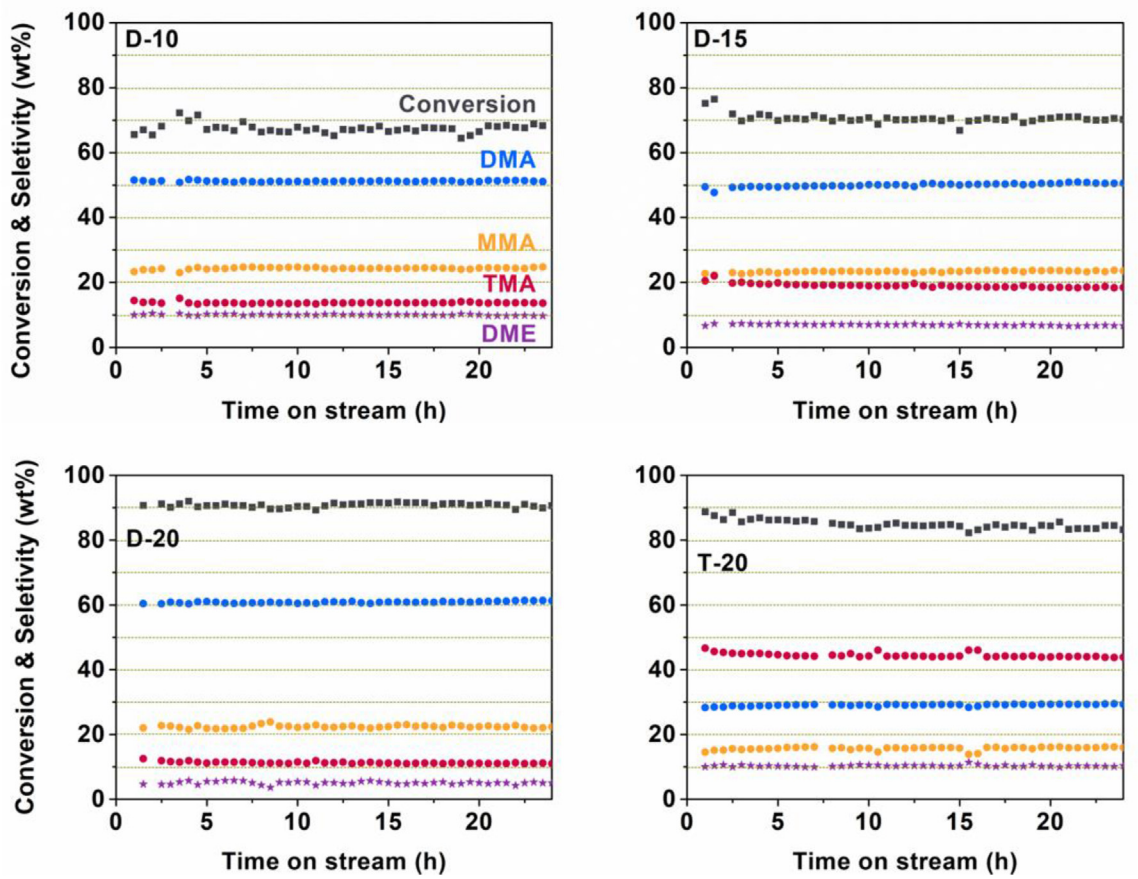

Fig. 6. Methanol conversion and product selectivities in the methanol amination reaction over SAPO-34. Reaction conditions: 320 °C, methanol WHSV = 0.813 h^{-1}, NH_3/CH_3OH = 2/1 (in mole).

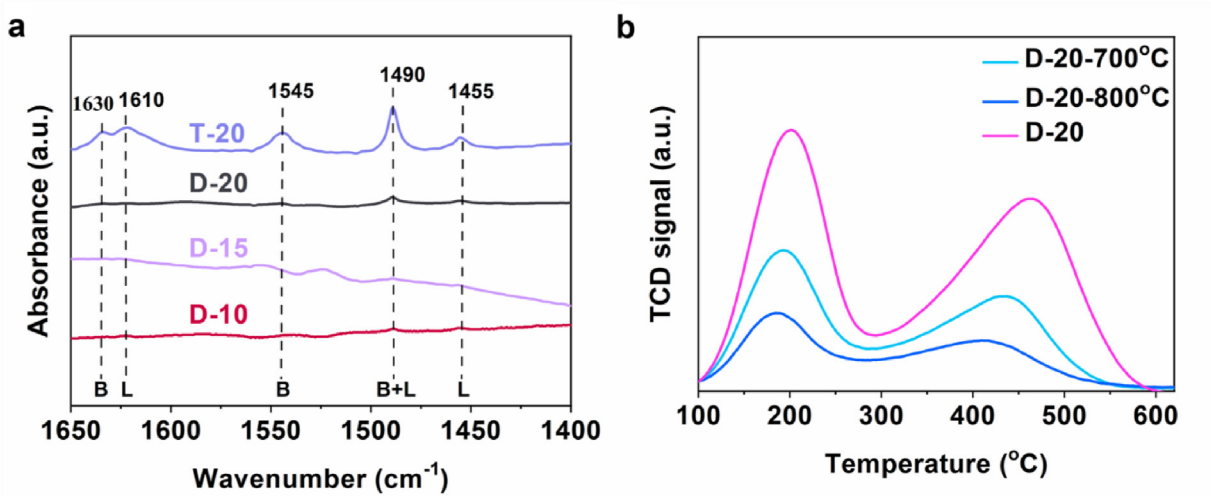

Fig. 7. (a) Pyridine-adsorbed FTIR spectra and (b) NH_3-TPD profiles of the samples. The hydrothermal aging was conducted under 100% steam at 700 °C (or 800 °C) for 13 h.

Table 5
The methanol amination reaction over sample D-20 after hydrothermal aging at 700 °C (or 800 °C) for 13 h[a].

Sample	Time (h)	Methanol conversion (%)	Selectivity (wt%)					
			MMA	DMA	TMA	DME	CH_4	MMA + DMA[b]
D-20	12	91.4	22.3	60.9	11.3	5.1	0	88.0
	20	90.8	22.7	61.0	11.1	5.1	0	88.3
D-20−700°C	12	82.2	25.0	64.3	5.2	5.0	0	95.4
	20	82.4	24.6	64.3	5.6	5.1	0	95.2
D-20−800°C	12	65.2	29.6	55.7	4.1	9.9	0	94.5
	20	67.0	28.9	56.2	4.3	9.9	0	94.1

[a] Methanol WHSV = 0.813 h^{-1}, NH_3/CH_3OH = 2/1 (in mole).
[b] The selectivity of (MMA + DMA) in three methylamines.

4. Conclusions

The spent industrial MTO catalyst has been demonstrated to be effective raw material for the synthesis of SAPO-34 molecular sieve. The physicochemical properties of the obtained SAPO-34 with varied Si contents are similar to those synthesized by conventional sources. More interestingly, low silica SAPO-34 behaves good catalytic performance for the MTO reaction, and high silica SAPO-34 synthesized by DEA template exhibits superior catalytic activity and selectivity of MMA plus DMA for the methanol ammoniation reaction. The obviously low (MMA + DMA) selectivity on SAPO-34 templated by TEAOH is caused by their small crystal sizes and high acid concentrations on the crystal surface. After high-temperature hydrothermal aging, although the acid concentration of SAPO-34-DEA shows a decrease and the methanol conversion drops, the (MMA + DMA) selectivity in the methylamines rises to as high as 94%, implying its potential as highly selective catalyst for methanol ammoniation reaction. The present work evidenced the high reactivity of the spent industrial MTO catalyst for SAPO synthesis and would facilitate its disposal and the development of MTO process.

Statement of contribution of co-authors

Zhao Liu: Investigation, Writing - Original Draft.
Quanyi Wang: Methodology, Validation, Discussion, Review & Editing.
Shiping Liu: Investigation.
Dong Fan: Investigation.
Miao Yang and Dali Zhu: Investigation, Discussion.
Peng Tian: Supervision, Conceptualization, Methodology, Writing - Review & Editing.
Zhongmin Liu: Supervision, Conceptualization, Writing - Review & Editing.
All authors have read and approved the final manuscript.

Declaration of competing interest

The authors declare that they have no known competing financial interests or personal relationships that could have appeared to influence the work reported in this paper.

Data availability

Data will be made available on request.

Acknowledgements

This work is supported by the National Natural Science Foundation of China (21991090, 21991091, 22171259), the Key Research Program of Frontier Sciences, CAS (QYZDB-SSW-JSC040).

Appendix A. Supplementary data

Supplementary data to this article can be found online at https://doi.org/10.1016/j.mtsust.2022.100302.

References

[1] U. Olsbye, S. Svelle, M. Bjrgen, P. Beato, T. Janssens, F. Joensen, S. Bordiga, K. Lillerud, Conversion of methanol to hydrocarbons: how zeolite cavity and pore size controls product selectivity, Angew. Chem. Int. Ed. 51 (2012) 5810–5831.

[2] P. Tian, Y. Wei, M. Ye, Z. Liu, Methanol to olefins (MTO): from fundamentals to commercialization, ACS Catal. 5 (2015) 1922–1938.

[3] W. Dai, X. Wang, G. Wu, N. Guan, M. Hunger, L. Li, Methanol-to-Olefin conversion on silicoaluminophosphate catalysts: effect of brnsted acid sites and framework structures, ACS Catal. 1 (2011) 292–299.

[4] W. Wei, M. Hunger, Reactivity of surface alkoxy species on acidic zeolite catalysts, Acc. Chem. Res. 39 (2008) 895–904.

[5] Y. Irina, C.A. Dutta, M. Florian, B. Weckhuysen, G. Jorge, Recent trends and fundamental insights in the methanol-to-hydrocarbons process, Nature Catalysis 1 (2018) 398–411.

[6] M. Yang, D. Fan, P. Tian, Y. Wei, Z.M. Liu, Recent progress in methanol-to-olefins (MTO) catalysts, Adv. Mater. 31 (2019), 1902181.

[7] S. Wilson, P. Barger, The characteristics of SAPO-34 which influence the conversion of methanol to light olefins, Microporous Mesoporous Mater. 29 (1999) 117–126.

[8] F. Guo, X. Wang, P. Wang, L. Xuan, Facile synthesis of SAPO-34 with excellent methanol-to-olefin activity in a short time via a conventional hydrothermal method, New J. Chem. 44 (2020) 10140–10417.

[9] Q. Sun, Z. Xie, J. Yu, The state-of-the-art synthetic strategies for SAPO-34 zeolite catalysts in methanol-to-olefin conversion, Natl. Sci. Rev. 4 (2018) 542–558.

[10] Y. Zhou, H. Shi, B. Wang, G. Chen, J. Yi, J. Li, The synthesis of SAPO-34 zeolite for an improved MTO performance: tuning the particle size and an insight into the formation mechanism, Inorg. Chem. Front. 8 (2021) 2315–2322.

[11] H. Jeon, C. Shin, H. Jung, S. Hong, Catalytic evaluation of small-pore molecular sieves with different framework topologies for the synthesis of methylamines, Appl. Catal. Gen. 305 (2006) 70–78.

[12] D. Corbin, S. Schwarz, G. Sonnichsen, Methylamines synthesis: a review, Catal. Today 37 (1997) 71–102.

[13] Y. Qiao, P. Wu, X. Xiang, M. Yang, Q. Wang, P. Tian, Z. Liu, SAPO-34 synthesized with n -butylamine as a template and its catalytic application in the methanol amination reaction, Chin. J. Catal. 38 (2017) 574–582.

[14] Y. Cao, D. Fan, D. Zhu, L. Sun, L. Cao, P. Tian, Z. Liu, The effect of Si environments on NH_3 selective catalytic reduction performance and moisture stability of Cu-SAPO-34 catalysts, J. Catal. 391 (2020) 404–413.

[15] J. Wang, T. Yu, X. Wang, G. Qi, J. Xue, M. Shen, L. Wei, The influence of silicon on the catalytic properties of Cu/SAPO-34 for NOx reduction by ammonia-SCR, Appl. Catal. B Environ. 127 (2012) 137–147.

[16] P. Wang, Z. Li, X. Wang, Y. Tong, F. Yuan, Y. Zhu, One-pot synthesis of Cu/SAPO-34 with hierarchical pore using cupric citrate as a copper source for excellent NH_3-SCR of NO performance, ChemCatChem 12 (2020) 4871–4878.

[17] L. Weng, W. Li, S. Schmieg, D. Wang, Role of Brønsted acidity in NH_3 selective catalytic reduction reaction on Cu/SAPO-34 catalysts, J. Catal. 324 (2015) 98–106.

[18] F. Dong, T. Peng, S. Xiong, Aminothermal synthesis of CHA-type SAPO molecular sieves and their catalytic performance in methanol to olefins (MTO) reaction, J. Mater. Chem. 1 (2013) 14206–14213.

[19] J. Yao, H. Tian, F. Zha, S. Ma, X. Tang, Y. Chang, X. Guo, Regulating the size and acidity of SAPO-34 zeolites using dual templates to enhance the selectivity of light olefins in MTO, New J. Chem. 45 (2021) 11812–11822.

[20] R. Vomscheid, M. Briend, M.J. Peltre, P. Man, D. Barthomeuf, The role of the template in directing the Si distribution in SAPO zeolites, J. Phys. Chem. 98 (1994) 9614–9618.

[21] T. Álvaro-MuñOz, C. Márquez-Álvarez, E. Sastre, Use of different templates on SAPO-34 synthesis: effect on the acidity and catalytic activity in the MTO reaction, Catal. Today 179 (2012) 27–34.

[22] A. Prakash, S. Unnikrishnan, Synthesis of SAPO-34: high silicon incorporation in the presence of morpholine as template, J. Chem. Soc. Faraday. Trans. 90 (1994) 2291–2296.

[23] G. Liu, P. Tian, J. Li, D. Zhang, F. Zhou, Z. Liu, Synthesis, characterization and catalytic properties of SAPO-34 synthesized using diethylamine as a template, Microporous Mesoporous Mater. 111 (2008) 143–149.

[24] W. Dai, G. Cao, L. Yang, G.J. Wu, M. Dyballa, M. Hunger, N.J. Guan, L.D. Li, Insights into the catalytic cycle and activity of methanol-to-olefin conversion over low-silica AlPO-34 zeolites with controllable Bronsted acid density, Catal. Sci. Technol. 7 (2017) 607–618.

[25] L. Xuan, X. Wang, Y. Zhu, Z. Li, Synthesis of low-silica SAPO-34 at lower hydrothermal temperature by additional pressure and its enhanced catalytic performance for methanol to olefin, Microporous Mesoporous Mater. 323 (2021), 111218.

[26] P. Rungrojchaipon, X. Wang, A.J. Jacobson, Crystal growth of AlPO-5, AlPO-15, and AlPO-21 from aluminum foil, Microporous Mesoporous Mater. 109 (2008) 478–484.

[27] A. Izadbakhsh, F. Farhadi, F. Khorasheh, S. Sahebdelfar, M. Asadi, Y.Z. Feng, Effect of SAPO-34's composition on its physico-chemical properties and deactivation in MTO process, Appl. Catal. Gen. 364 (2009) 48–56.

[28] P. Tian, B. Li, S. Xu, X. Su, D. Wang, L. Zhang, D. Fan, Y. Qi, Z. Liu, Investigation of the crystallization process of SAPO-35 and Si distribution in the crystals, J. Phys. Chem. C 117 (2013) 4048–4056.

[29] G. Liu, P. Tian, Z. Liu, Synthesis of SAPO-34 molecular sieves templated with diethylamine and their properties compared with other templates, Chin. J. Catal. 33 (2012) 174–182.

[30] D. Fan, P. Tian, S. Xu, Q. Xia, X. Su, L. Zhang, Y. Zhang, Y. He, Z. Liu, A novel solvothermal approach to synthesize SAPO molecular sieves using organic amines as the solvent and template, J. Mater. Chem. 22 (2012) 6568–6574.

[31] N. Nasim, S. Askari, R. Halladj, Hydrothermal synthesis of nanosized SAPO-34 molecular sieves by different combinations of multi templates, Powder Technol. 254 (2014) 324–330.

[32] C. Liu, Z. Liu, L. Yang, G. Gai, Adjusting the crystallite size of SAPO-34 molecular sieve by the dual template method, J. Mol. Catal. 8 (3) (1994) 207–212.

[33] N. Yan, H. Xu, W. Zhang, T. Sun, P. Guo, P. Tian, Z. Liu, Probing locations of organic structure-directing agents (OSDAs) and host-guest interactions in CHA -type SAPO-34/44, Microporous Mesoporous Mater. 264 (2018) 55–59.

[34] P. Wu, M. Yang, W. Zhang, S. Xu, P. Guo, P. Tian, Z. Liu, Synthesis of SAPO-34 nanoaggregates with the assistance of an inexpensive three-in-one non-surfactant organosilane, Chem. Commun. 53 (2017) 4985–4988.

[35] P. Wu, M. Yang, W. Zhang, S. Zeng, M. Gao, S. Xu, P. Tian, Z. Liu, Silicoaluminophosphate molecular sieve DNL-6: synthesis with a novel template, N,N′-dimethylethylenediamine, and its catalytic application, Chin. J. Catal. 39 (2018) 1511–1519.